



LAWRENCE
LIVERMORE
NATIONAL
LABORATORY

LLNL-TR-648225

Three Analytic Benchmarks in COG

Edward M. Lent

January 9, 2014

Disclaimer

This document was prepared as an account of work sponsored by an agency of the United States government. Neither the United States government nor Lawrence Livermore National Security, LLC, nor any of their employees makes any warranty, expressed or implied, or assumes any legal liability or responsibility for the accuracy, completeness, or usefulness of any information, apparatus, product, or process disclosed, or represents that its use would not infringe privately owned rights. Reference herein to any specific commercial product, process, or service by trade name, trademark, manufacturer, or otherwise does not necessarily constitute or imply its endorsement, recommendation, or favoring by the United States government or Lawrence Livermore National Security, LLC. The views and opinions of authors expressed herein do not necessarily state or reflect those of the United States government or Lawrence Livermore National Security, LLC, and shall not be used for advertising or product endorsement purposes.

Auspices

This work performed under the auspices of the U.S. Department of Energy by Lawrence Livermore National Laboratory under Contract DE-AC52-07NA27344.

Three analytic benchmarks in COG

Analytic benchmarks are valuable tools to test the algorithms in Monte Carlo codes not related to geometry or interaction data. COG [1,2,3] was used to calculate three analytic benchmarks: Kobayashi's benchmarks for simple geometries and void regions [4]; Shmakov's benchmarks using the back-and-forth approximation [5]; and Thomas et al's critical problem for an infinite cylinder [6].

1) The Kobayashi benchmarks

The Kobayashi [4] benchmarks are a set of three problems, each consisting of three regions – source, void, and shield (void is actually shield with a density multiplier of 0.001). Problem 1 is a shield with square void, Problem 2 is a shield with void duct, and Problem 3 is a shield with dog-leg void duct. See reference [4] for the exact geometries. Fluxes were determined at various points through out the geometry. The analytic results are obtained for pure absorber shield. The Monte Carlo code COG was used to redo the benchmark calculations.

Results for Problem 1 – shield with square void

x,y,z	Analytic	COG	COG/Analytic
5,5,5	5.95659E+0	5.9537E+0 ± 1.48E-2	0.99952 ± 0.00250
5,15,5	1.37185E+0	1.3718E+0 ± 6.74E-5	0.99996 ± 0.00005
5,25,5	5.00871E-1	5.0086E-1 ± 1.55E-5	0.99998 ± 0.00003
5,35,5	2.52429E-1	2.5242E-1 ± 6.66E-6	0.99996 ± 0.00003
5,45,5	1.50260E-1	1.5026E-1 ± 3.64E-6	1.00000 ± 0.00002
5,55,5	5.95286E-2	5.9530E-2 ± 1.36E-6	1.00002 ± 0.00002
5,65,5	1.53283E-2	1.5328E-2 ± 3.34E-7	0.99998 ± 0.00002
5,75,5	4.17689E-3	4.1769E-3 ± 8.85E-8	1.00000 ± 0.00002
5,85,5	1.18533E-3	1.1854E-3 ± 2.44E-8	1.00006 ± 0.00002
5,95,5	3.46846E-4	3.4686E-4 ± 7.01E-9	1.00004 ± 0.00002

Table 1. The analytic and COG flux results for Problem 1A

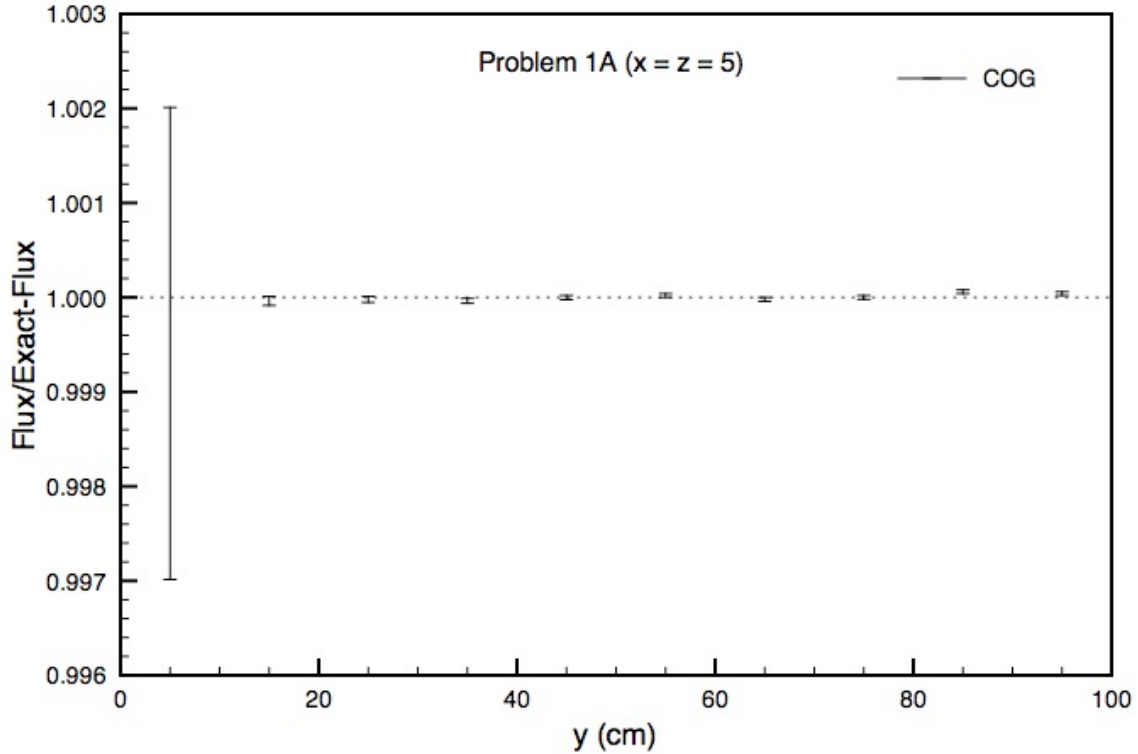


Figure 1. The results for Problem 1A as the ratio of the COG flux to analytic flux

x,y,z	Analytic	COG	COG/Analytic
5,5,5	5.95659E+0	5.9537E+0 ± 1.49E-2	0.99952 ± 0.00250
15,15,15	4.70754E-1	4.7083E-1 ± 5.84E-5	1.00016 ± 0.00012
25,25,25	1.69968E-1	1.6998E-1 ± 1.36E-5	1.00007 ± 0.00008
35,35,35	8.68334E-2	8.6838E-2 ± 6.05E-6	1.00005 ± 0.00007
45,45,45	5.25132E-2	5.2515E-2 ± 3.41E-6	1.00003 ± 0.00007
55,55,55	1.33378E-2	1.3338E-2 ± 8.27E-7	1.00001 ± 0.00006
65,65,65	1.45867E-3	1.4587E-3 ± 8.83E-8	1.00002 ± 0.00006
75,75,75	1.75364E-4	1.7537E-4 ± 1.05E-8	1.00003 ± 0.00006
85,85,85	2.24607E-5	2.2462E-5 ± 1.34E-9	1.00006 ± 0.00006
95,95,95	3.01032E-6	3.0105E-6 ± 1.8E-10	1.00006 ± 0.00006

Table 2. The analytic and COG flux results for Problem 1B

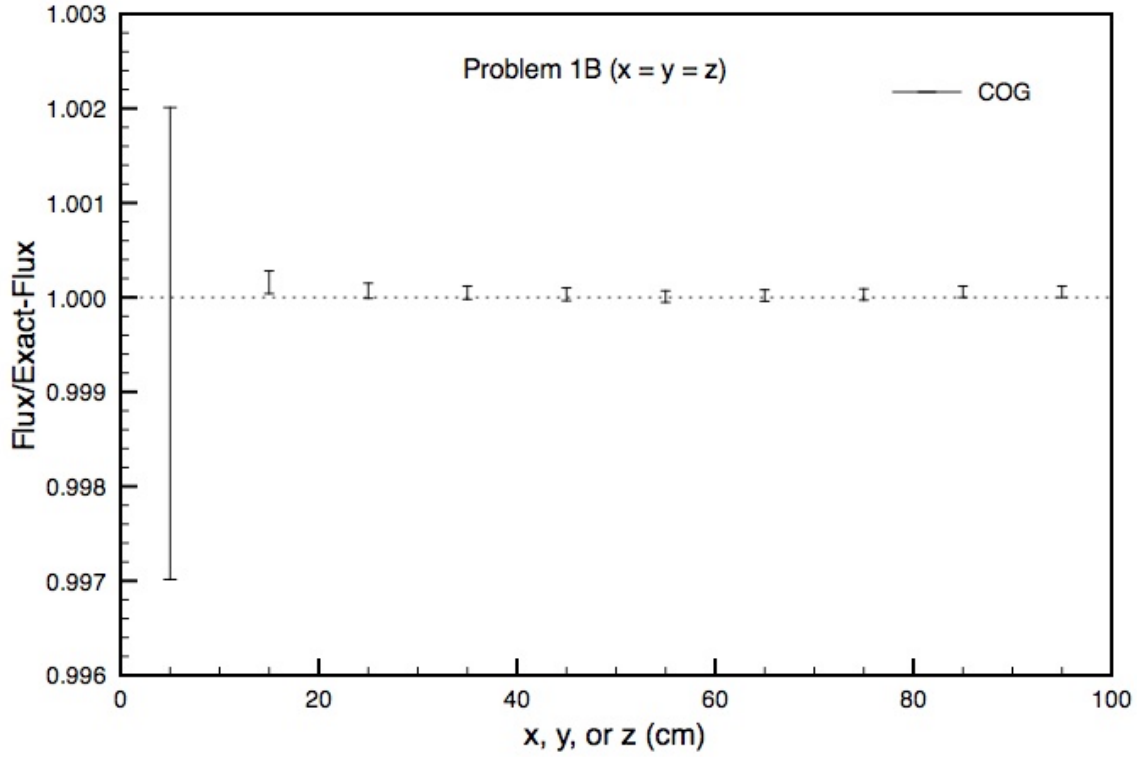


Figure 2. The results for Problem 1B as the ratio of the COG flux to analytic flux

x,y,z	Analytic	COG	COG/Analytic
5,55,5	5.95290E-2	5.9530E-2 ± 4.50E-6	1.00000 ± 0.00008
15,55,5	5.50250E-2	5.5026E-2 ± 4.09E-6	1.00000 ± 0.00007
25,55,5	4.80750E-2	4.8077E-2 ± 3.47E-6	1.00000 ± 0.00007
35,55,5	3.96770E-2	3.9677E-2 ± 2.80E-6	1.00000 ± 0.00007
45,55,5	3.16370E-2	3.1637E-2 ± 2.19E-6	1.00000 ± 0.00007
55,55,5	2.35300E-2	2.3530E-2 ± 1.59E-6	0.99999 ± 0.00007
65,55,5	5.83720E-3	5.8372E-3 ± 3.98E-7	1.00000 ± 0.00007
75,55,5	1.56730E-3	1.5673E-3 ± 1.06E-7	0.99999 ± 0.00007
85,55,5	4.53110E-4	4.5311E-4 ± 3.04E-8	0.99999 ± 0.00007
95,55,5	1.37080E-4	1.3708E-4 ± 9.10E-9	1.00000 ± 0.00007

Table 3. The analytic and COG flux results for Problem 1C

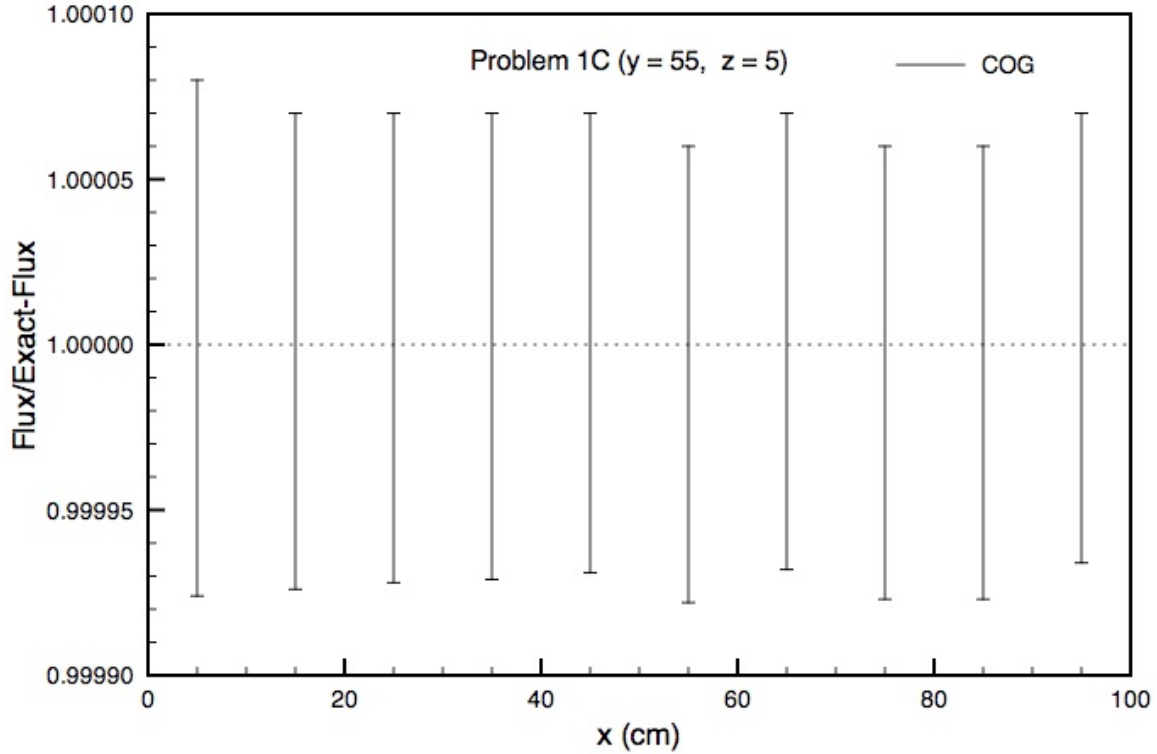


Figure 3. The results for Problem 1C as the ratio of the COG flux to analytic flux

Results for Problem 2 – shield with void duct

x,y,z	Analytic	COG	COG/Analytic
5,5,5	5.95659E+0	5.9510E+0 ± 1.57E-2	0.99900 ± 0.00263
5,15,5	1.37185E+0	1.3717E+0 ± 2.24E-4	0.99989 ± 0.00016
5,25,5	5.00871E-1	5.0088E-1 ± 5.11E-5	1.00002 ± 0.00010
5,35,5	2.52429E-1	2.5244E-1 ± 2.21E-5	1.00004 ± 0.00009
5,45,5	1.50260E-1	1.5027E-1 ± 1.21E-5	1.00007 ± 0.00008
5,55,5	9.91726E-2	9.9176E-2 ± 7.51E-6	1.00003 ± 0.00008
5,65,5	7.01791E-2	7.0182E-2 ± 5.10E-6	1.00004 ± 0.00007
5,75,5	5.22062E-2	5.2208E-2 ± 3.68E-6	1.00003 ± 0.00007
5,85,5	4.03188E-2	4.0320E-2 ± 2.77E-6	1.00003 ± 0.00007
5,95,5	3.20574E-2	3.2059E-2 ± 2.16E-6	1.00005 ± 0.00007

Table 4. The analytic and COG flux results for Problem 2A

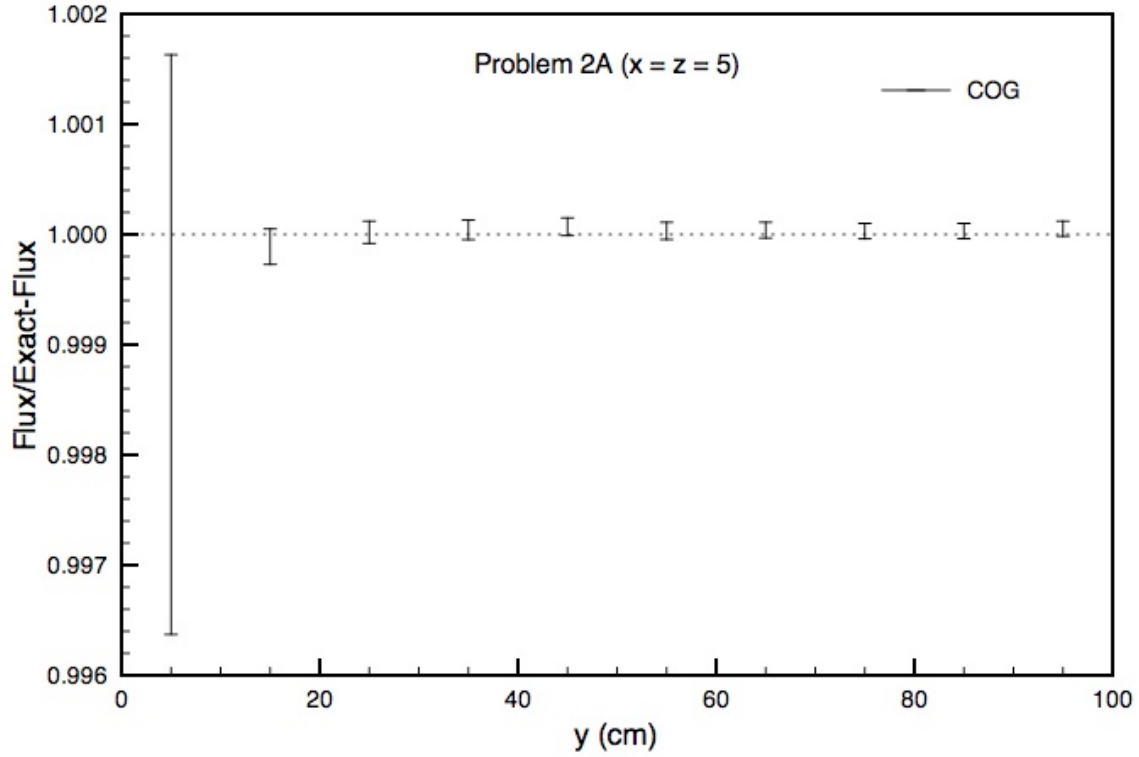


Figure 4. The results for Problem 2A as the ratio of the COG flux to analytic flux

x,y,z	Analytic	COG	COG/Analytic
5,95,5	3.20574E-2	3.2058E-2 ± 2.16E-6	1.00002 ± 0.00007
15,95,5	1.70541E-3	1.7053E-3 ± 2.27E-7	0.99994 ± 0.00013
25,95,5	1.40557E-4	1.4055E-4 ± 2.09E-8	0.99995 ± 0.00015
35,95,5	3.27058E-5	3.2704E-5 ± 4.68E-9	0.99995 ± 0.00014
45,95,5	1.08505E-5	1.0851E-5 ± 1.44E-9	1.00000 ± 0.00013
55,95,5	4.14132E-6	4.1412E-6 ± 5.1E-10	0.99997 ± 0.00012

Table 5. The analytic and COG flux results for Problem 2B

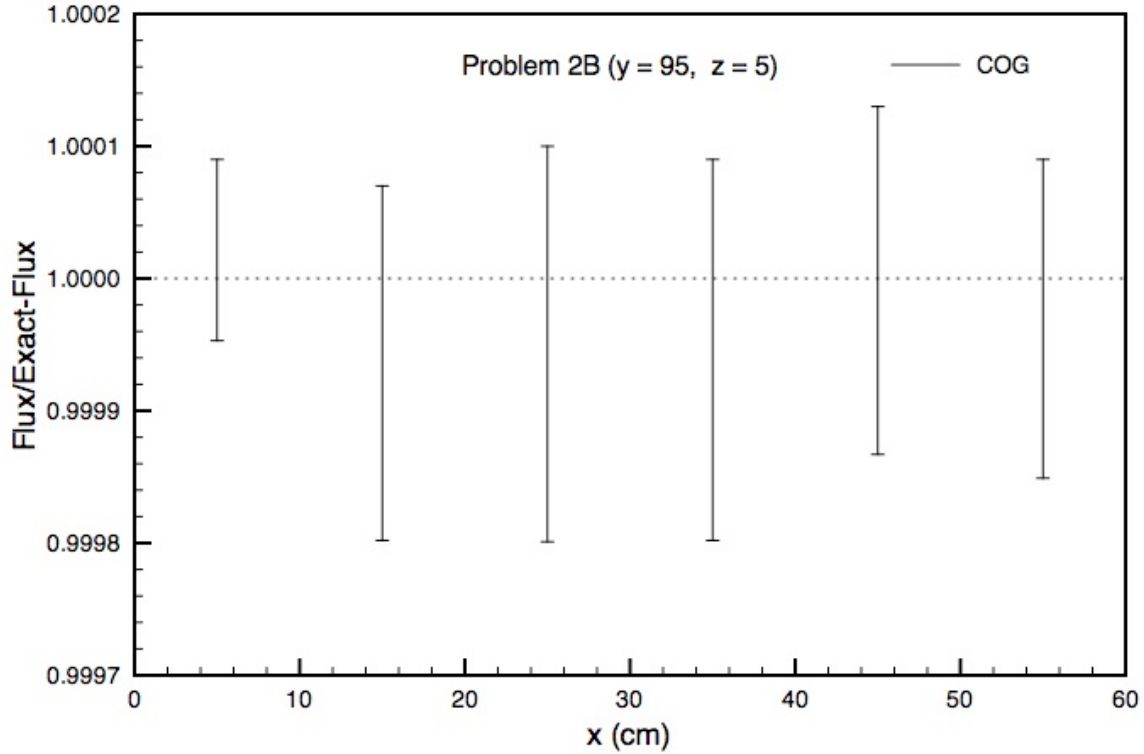


Figure 5. The results for Problem 2B as the ratio of the COG flux to analytic flux

Results for Problem 3 – shield with dog-leg void duct

x,y,z	Analytic	COG	COG/Analytic
5,5,5	5.95659E+0	5.9524E+0 ± 8.93E-3	0.99930 ± 0.00150
5,15,5	1.37185E+0	1.3720E+0 ± 2.24E-4	1.00011 ± 0.00016
5,25,5	5.00871E-1	5.0093E-1 ± 5.11E-5	1.00012 ± 0.00010
5,35,5	2.52429E-1	2.5246E-1 ± 2.21E-5	1.00012 ± 0.00009
5,45,5	1.50260E-1	1.5028E-1 ± 1.21E-5	1.00013 ± 0.00008
5,55,5	9.91726E-2	9.9185E-2 ± 7.51E-6	1.00013 ± 0.00008
5,65,5	4.22623E-2	4.2267E-2 ± 3.06E-6	1.00011 ± 0.00007
5,75,5	1.14703E-2	1.1472E-2 ± 8.05E-7	1.00015 ± 0.00007
5,85,5	3.24662E-3	3.2470E-3 ± 2.22E-7	1.00012 ± 0.00007
5,95,5	9.48324E-4	9.4844E-4 ± 6.36E-8	1.00012 ± 0.00007

Table 6. The analytic, and COG flux results for Problem 3A

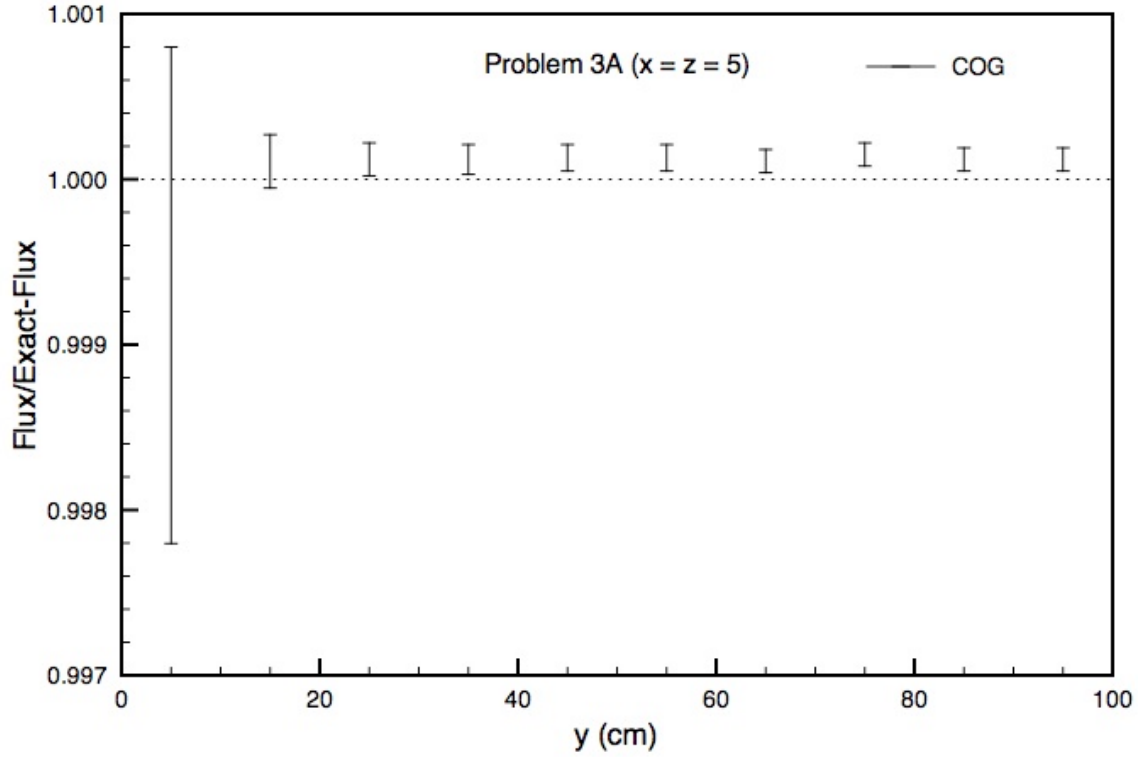


Figure 6. The results for Problem 3A as the ratio of the COG flux to analytic flux

x,y,z	Analytic	COG	COG/Analytic
5,55,5	9.91726E-2	9.9172E-2 \pm 7.51E-6	0.99999 \pm 0.00008
15,55,5	2.45041E-2	2.4503E-2 \pm 2.82E-6	0.99996 \pm 0.00012
25,55,5	4.54477E-3	4.5445E-3 \pm 5.45E-7	0.99994 \pm 0.00012
35,55,5	1.42960E-3	1.4295E-3 \pm 1.60E-7	0.99993 \pm 0.00011
45,55,5	2.64846E-4	2.6483E-4 \pm 2.70E-8	0.99994 \pm 0.00010
55,55,5	9.14210E-5	9.1418E-5 \pm 8.40E-9	0.99997 \pm 0.00009

Table 7. The analytic and COG flux results for Problem 3B

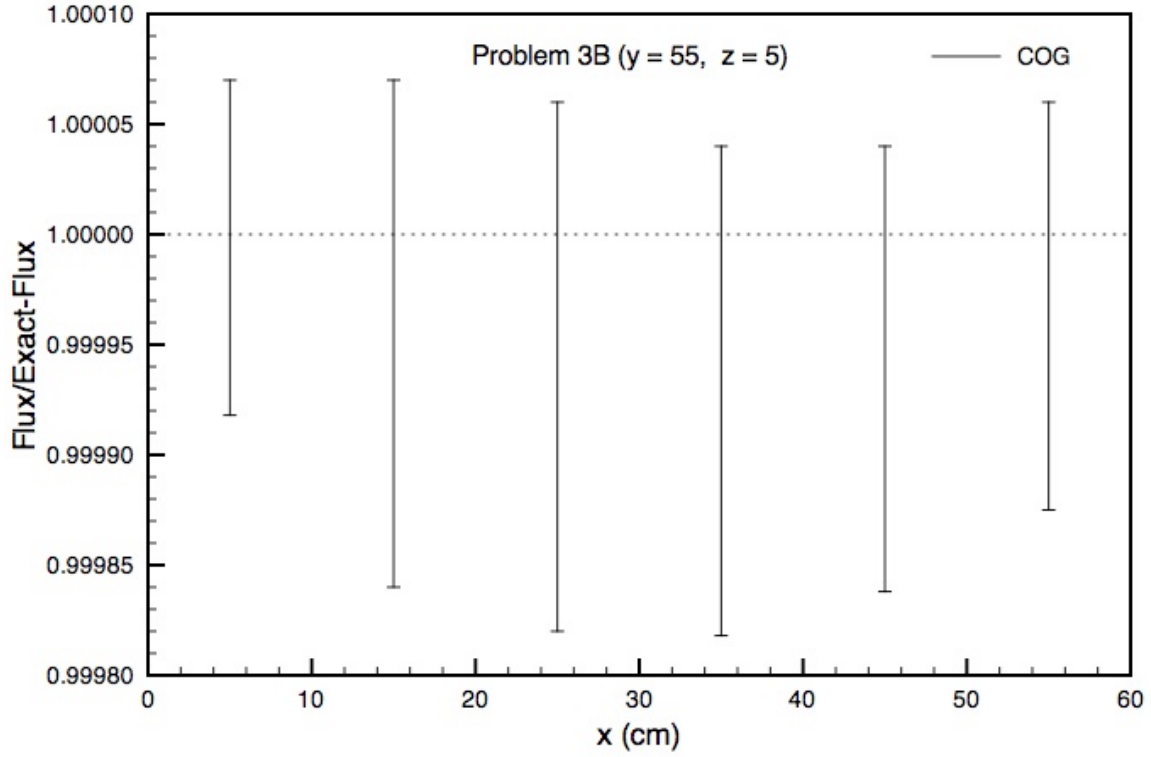


Figure 7. The results for Problem 3B as the ratio of the COG flux to analytic flux

x,y,z	Analytic	COG	COG/Analytic
5,95,35	3.27058E-5	3.2701E-5 \pm 4.68E-9	0.99985 \pm 0.00014
15,95,35	2.68415E-5	2.6837E-5 \pm 4.00E-9	0.99983 \pm 0.00015
25,95,35	1.70019E-5	1.6999E-5 \pm 2.70E-9	0.99983 \pm 0.00016
35,95,35	3.37981E-5	3.3791E-5 \pm 4.97E-9	0.99979 \pm 0.00015
45,95,35	6.04893E-6	6.0480E-6 \pm 8.2E-10	0.99985 \pm 0.00014
55,95,35	3.36460E-6	3.3642E-6 \pm 3.0E-10	0.99988 \pm 0.00009

Table 8. The analytic, and COG flux results for Problem 3C

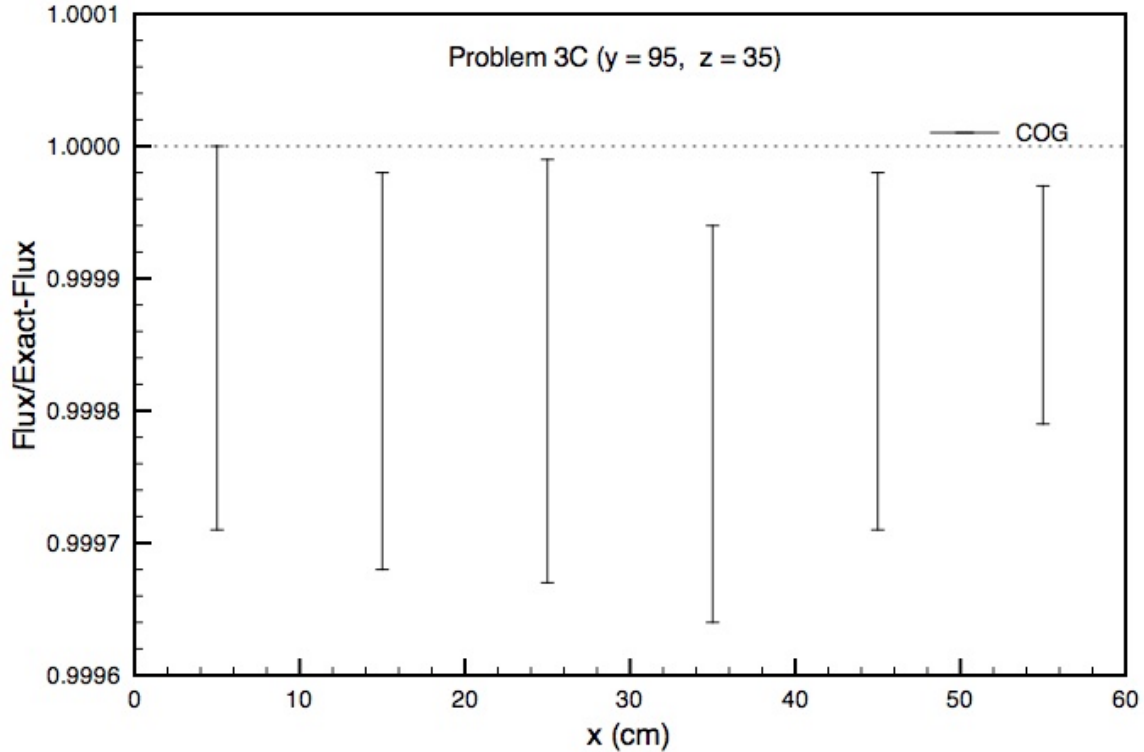


Figure 8. The results for Problem 3C as the ratio of the COG flux to analytic flux

Conclusions

The COG results are in excellent agreement with Kobayashi's analytic results.

2) The Back-and-forth Approximation

As described by Shmakov [5] the back-and-forth approximation is a simple neutron transport model that leads to analytic solutions for fissile systems in 1D geometries. The assumptions are threefold: 1) one group cross sections; 2) 1D geometries - planar, cylindrical, or spherical; and 3) neutrons are allowed to move only in *back and forth* directions, i.e. normal to the plane, cylinder, or sphere.

Results

A one-group cross section set for ^{235}U as described in Table 1 of reference [5] was developed for the Monte Carlo code COG.

σ_s	6.47 bn	scattering cross section
q	0.1	probability of back scatter for σ_s
σ_a	0.13 bn	absorption cross section
σ_f	1.25 bn	fission cross section
	0.5	probability of back scatter for σ_f
ν_f	2.6	neutrons per fission
E	1 MeV	neutron energy
v	$138 \text{ cm}/10^{-7} \text{ s}$	neutron velocity

COG calculations are compared to Shmakov's analytic results.

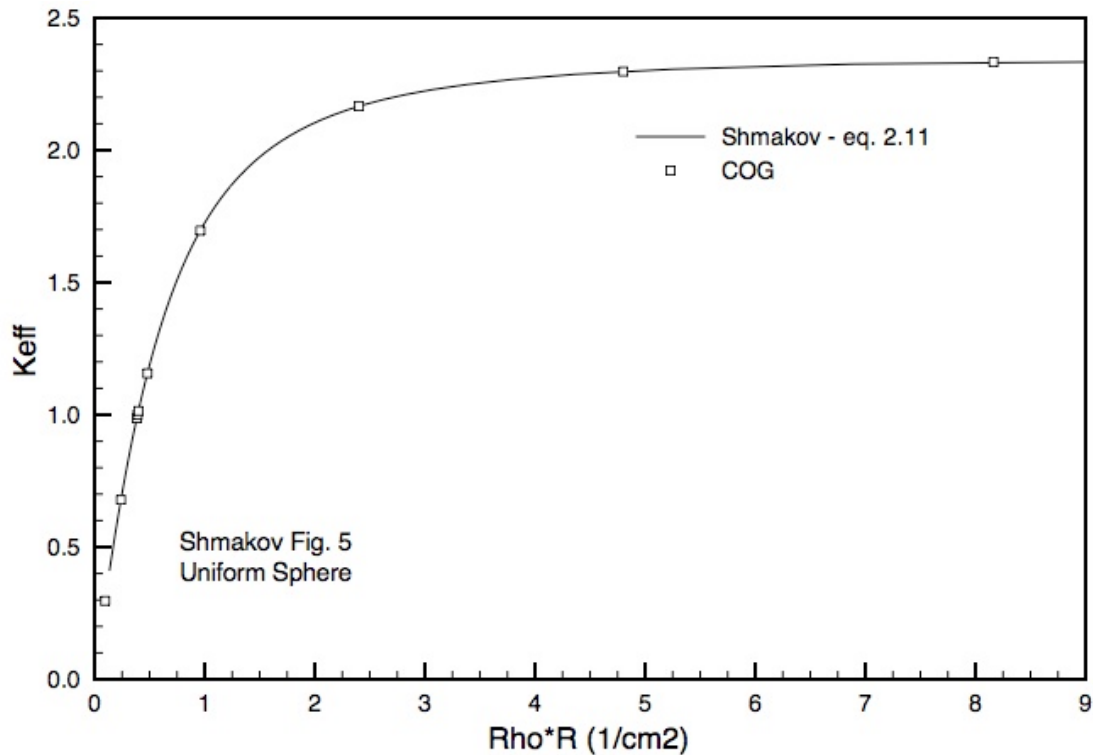


Figure 9. COG results for k_{eff} versus radius, $\rho \cdot R$, for a uniform sphere, compared with the analytic results of Shmakov, eq. 2.11

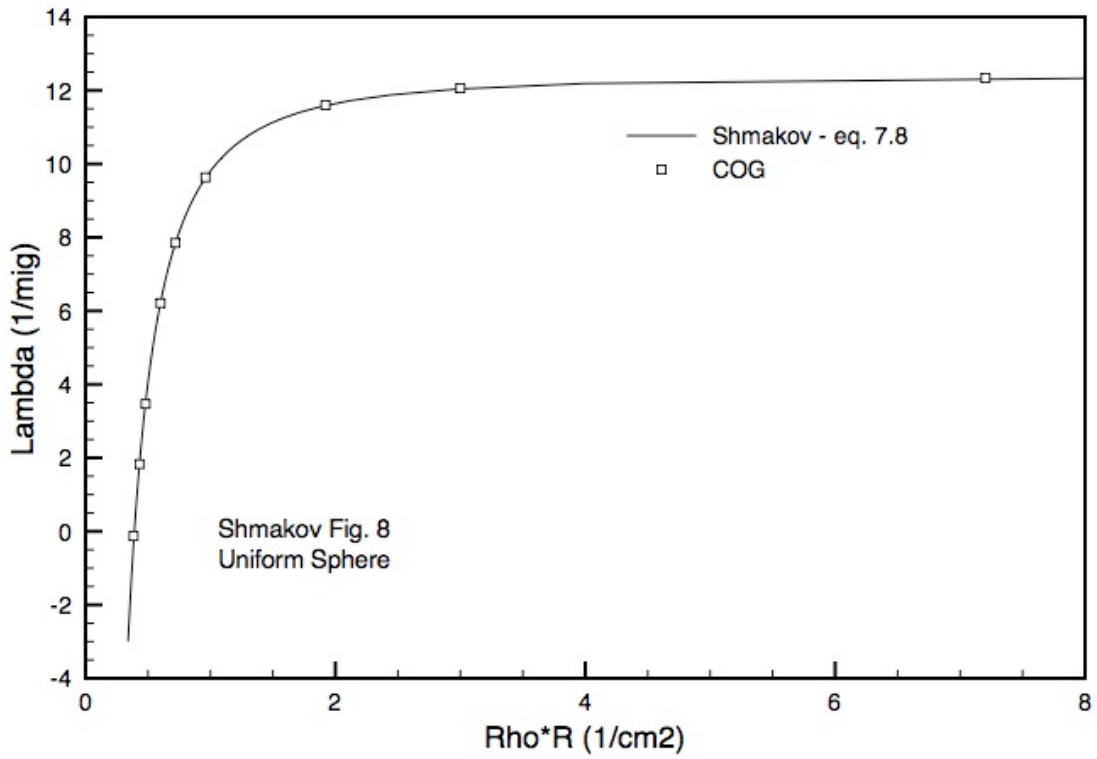


Figure 10. COG results for λ versus radius, ρ^*R , for a uniform sphere, compared with the analytic results of Shmakov, eq. 7.8

Note: Shmakov's λ is equivalent to COG's $\alpha/10$, where α is given in generations/ μ sec.

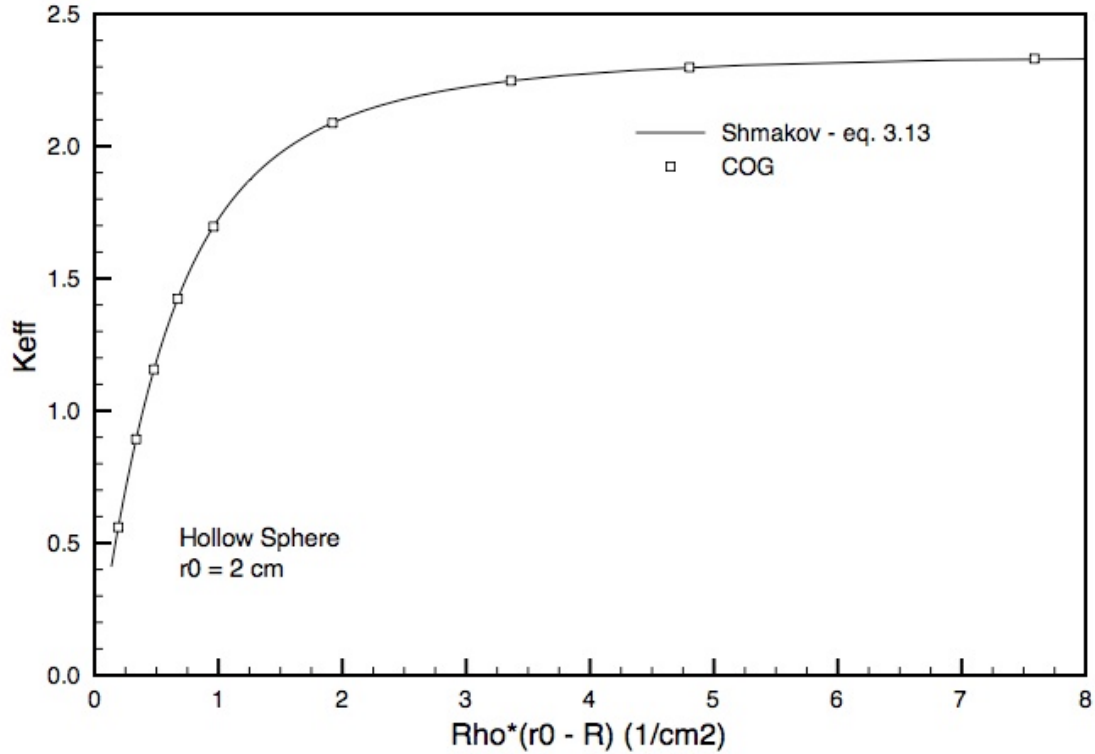


Figure 11. COG results for k_{eff} versus radius, $\rho^*(r_0 - R)$, for a hollow sphere, compared with the analytic results of Shmakov, eq. 3.13

	Analytic	COG	COG/Analytic
Leakage	1.3234298	1.32335 ± 0.00009	0.99994 ± 0.00007
Scattered	5.9850792	5.98491 ± 0.00019	0.99996 ± 0.00003
Fissioned	1.1563136	1.15637 ± 0.00007	1.00005 ± 0.00006
Absorbed	0.1202566	0.12025 ± 0.00003	0.99995 ± 0.00025
Collided	7.2616495	7.26153 ± 0.00022	0.99998 ± 0.00003
ν_f	2.6	2.60002	1.00001
k_{eff}	1.1563136	1.15637 ± 0.00007	1.00005 ± 0.00006

Table 9. Standard COG scores from a k_{eff} calculation for a hollow sphere with $r_0 = 2$ cm and $R = 12$ cm

The calculation was made using the above uranium cross section with $3 \cdot 10^7$ particle histories. The scores, normalized to one fission event by COG, have

been renormalized to k_{eff} to compare with the analytic results given in Table 2 from reference [5].

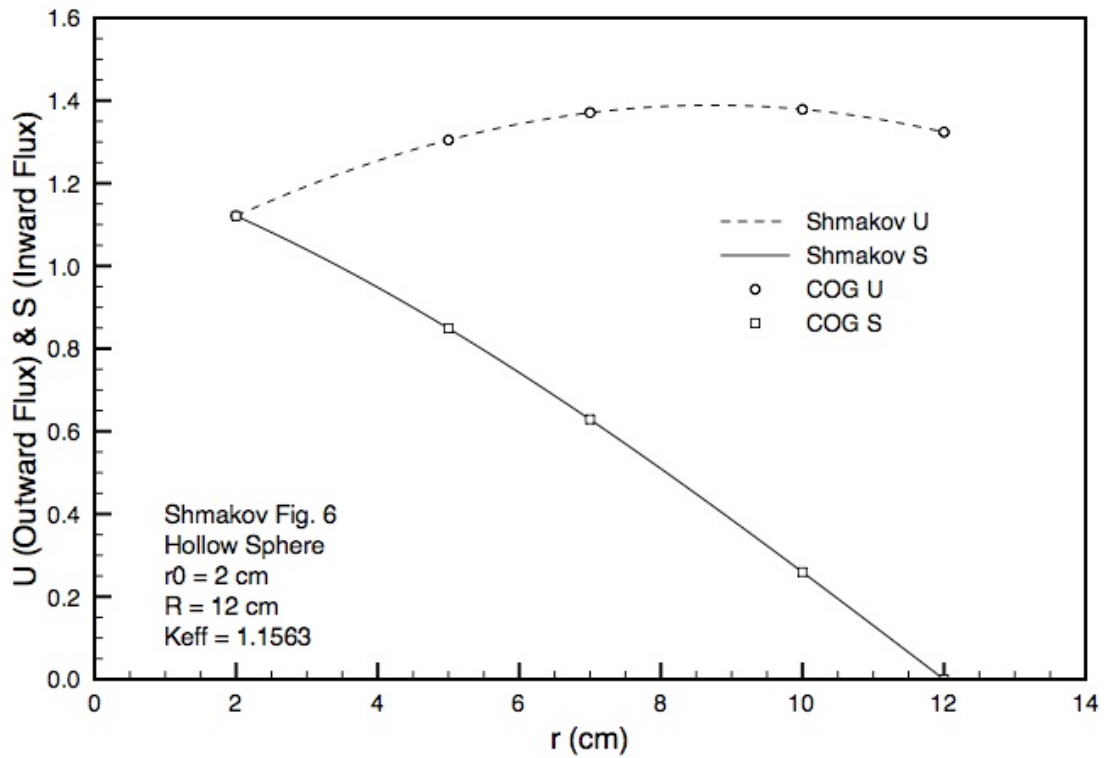


Figure 12. The outward flux, U , and the inward flux, S , as a function of radius in the $r_0 = 2$ cm, $R = 12$ cm hollow uranium sphere, compared with the analytic results of Shmakov, eqs. 3.11 and 3.12

Conclusions

It is seen the COG Monte Carlo one group cross section results agree excellently with the analytic results.

3) The infinite cylinder

Thomas et al [6] used the F_N method to compute the critical radius for a bare cylinder of infinite length. We use the Monte Carlo code COG to reproduce these results.

Results

A series of one group cross sections were generated for COG with $\Sigma_{\text{tot}} = 1/\text{cm}$, isotropic scattering, and $c = 1.01, 1.02, 1.05, 1.1, 1.2, 1.3, 1.4, 1.5, 1.6, 1.8,$ and 2.0 , where c is the mean number of secondary neutrons per collision. Then, for each c , COG was run in the criticality mode to compute k_{eff} as a function of radius to determine the critical radius. The results are shown in Table 10.

c	Thomas et al	COG	Ratio
1.01	13.12551647	13.129000	1.00027
1.02	9.04325484	9.071907	1.00317
1.05	5.41128828	5.406602	0.99913
1.1	3.57739129	3.576979	0.99988
1.2	2.28720926	2.287167	0.99998
1.3	1.72500292	1.724991	0.99999
1.4	1.39697859	1.396939	0.99997
1.5	1.17834084	1.178302	0.99997
1.6	1.02083901	1.020835	1.00000
1.8	0.80742662	0.807410	0.99998
2	0.66861286	0.668612	1.00000

Table 10. Compares the critical radius versus c

The flux versus radius was determined for $c = 1.05$ and 2 , the results are shown in Tables 11 and 12.

r/R	Thomas et al	COG	Ratio
0	1.000000	1.00450 ± 0.01552	1.00450 ± 0.01552
0.25	0.929851	0.93038 ± 0.00049	1.00060 ± 0.00053
0.5	0.733990	0.73366 ± 0.00031	0.99955 ± 0.00042
0.75	0.452168	0.45185 ± 0.00018	0.99929 ± 0.00039
0.85	0.326662	0.32666 ± 0.00015	1.00000 ± 0.00045
0.91	0.249166	0.24913 ± 0.00012	0.99987 ± 0.00047
0.95	0.195805	0.19581 ± 0.00010	1.00000 ± 0.00050
0.98	0.153085	0.15315 ± 0.00009	1.00040 ± 0.00056
1	0.117908	0.11800 ± 0.00005	1.00070 ± 0.00042

Table 11. Compares the flux versus radius with $c = 1.05$

r/R	Thomas et al	COG	Ratio
0	1.000000	0.98526 ± 0.03887	0.98526 ± 0.03887
0.25	0.959783	0.96013 ± 0.00046	1.00036 ± 0.00048
0.5	0.842634	0.84248 ± 0.00029	0.99981 ± 0.00034
0.75	0.656963	0.65718 ± 0.00019	1.00033 ± 0.00029
0.85	0.564397	0.56425 ± 0.00015	0.99974 ± 0.00027
0.91	0.502561	0.50261 ± 0.00013	1.00009 ± 0.00026
0.95	0.457217	0.45700 ± 0.00011	0.99953 ± 0.00024
0.98	0.418991	0.41896 ± 0.00009	0.99993 ± 0.00022
1	0.386649	0.38672 ± 0.00005	1.00017 ± 0.00014

Table 12. Compares the flux versus radius with $c = 2$

Conclusions

Again the COG Monte Carlo results are in excellent agreement with the analytic results.

References

- [1] R.M. Buck, E. M. Lent, *COG User's Manual: A Multiparticle Monte Carlo Transport Code*, Lawrence Livermore National Laboratory, Livermore CA, UCRL-TM-202590, 5th Edition (Sept. 1, 2002).
- [2] R.M. Buck, E. M. Lent, *COG11 Manual Supplement*, Lawrence Livermore National Laboratory, Livermore CA, LLNL-SM-461824 (Nov. 8, 2010)
- [3] R.M. Buck, E. M. Lent, *COG11.1 Manual Supplement*, Lawrence Livermore National Laboratory, Livermore CA, LLNL-SM-635621 (April. 15, 2013)
- [4] Kobayashi, K., Sugimura, N., and Nagaya, Y., *3-D Radiation Transport Benchmark Problems and Results for Simple Geometries with Void Regions*, Nuclear Energy Agency, Report NSC-DOC2000-4 (2000)
- [5] V. M. Shmakov, *Back-and-forth approximation, k_{eff} and λ* , Russian Federal Nuclear Center – (RFNC-VNIITF).

[6] J. R. Thomas, Jr., J. D. Southers, and C. E. Siewert, *Nucl. Sci. Eng.*, **84**, 79-82 (1983)